Inorganic Chemistry
Article

Inorg. Chem. **2009**, *48*, 5697–5703 **5697**
DOI: 10.1021/ic802125z

Biphenolate Phosphine Complexes of Tantalum

Lan-Chang Liang,*,† Liang-Chien Cheng,† Tzung-Ling Tsai,† Ching-Han Hu,‡ and Wen-Hsin Guo‡

†*Department of Chemistry and Center for Nanoscience & Nanotechnology, National Sun Yat-sen University, Kaohsiung 80424, Taiwan, and* ‡*Department of Chemistry, National Changhua University of Education, Changhua 50058, Taiwan*

Received November 5, 2008

The preparation and structural characterization of tantalum complexes supported by 2,2′-phenylphosphino-bis(4,6-di-*tert*-butylphenolate) ($[OPO]^{2-}$) are described. The reaction of $Li_2[OPO]$ with $TaCl_5$, regardless of the molar ratio employed, in diethyl ether at −35 °C led to high-yield isolation of yellow crystalline $[OPO]_2TaCl$. Alkylation of $[OPO]_2TaCl$ with MeMgBr or EtMgCl in diethyl ether at −35 °C generated the corresponding alkyl complexes $[OPO]_2TaR$ (R = Me, Et). Thermolysis of $[OPO]_2TaEt$ in benzene led to quantitative formation of $[OPO]_2TaH$, which could also be prepared by treatment of $[OPO]_2TaCl$ with $LiHBEt_3$ in diethyl ether at −35 °C. Hydrolysis of $[OPO]_2TaCl$ or $[OPO]_2TaR$ (R = H, Me, Et) generated $[OPO]_2TaOH$. The reaction of $[OPO]_2TaOH$ with Me_3SiCl in diethyl ether at room temperature afforded quantitatively $[OPO]_2TaCl$. The solution structures of these complexes were all characterized by multinuclear NMR spectroscopy. The solid-state structures of $[OPO]_2TaCl$, $[OPO]_2TaH$, and $[OPO]_2TaOH$ were determined by X-ray crystallography. The spectroscopic and crystallographic data are all indicative of the coordination of both phosphorus donors to tantalum in these 7-coordinate complexes. Interestingly, the structure of $[OPO]_2TaH$ is markedly different from those of $[OPO]_2TaX$ (X = Cl, OH, Me, Et) on the basis of NMR and X-ray studies. Density functional theory computations reveal that the hydride structure found by X-ray crystallography is lower in energy by about 7 kcal/mol than that analogous to the established X-ray structures of $[OPO]_2TaCl$ and $[OPO]_2TaOH$.

Introduction

We are currently exploring the coordination chemistry of main-group and transition metals involving *o*-phenylene-derived hybrid chelating ligands **1** and **2** (Figure 1) that contain both soft and hard donors.[1−18] Ligands of these types have shown to bind to both hard and soft metals as anticipated from the standpoint of the hard and soft acids and bases theory. It has been demonstrated that the rigidity imposed by the *o*-phenylene backbone in these ligands is beneficial in view of the inhibited propensity of donor atom dissociation and the enhanced thermal stability of derived metal complexes.[3,5,9−11,18]

Studies by Fryzuk and co-workers revealed that early transition metal complexes of **3** and **4** are capable of dinitrogen activation.[19−23] Of particular interest is the functionalization of dinitrogen molecules by zirconium or tantalum complexes.[22−26] The phenolate ligands **2** and amido ligands **3**

*To whom correspondence should be addressed. E-mail: lcliang@mail.nsysu.edu.tw.

(1) Liang, L.-C. *Coord. Chem. Rev*. **2006**, *250*, 1152–1177.
(2) Chien, P.-S.; Liang, L.-C. *Inorg. Chem*. **2005**, *44*, 5147–5151.
(3) Huang, M.-H.; Liang, L.-C. *Organometallics* **2004**, *23*, 2813–2816.
(4) Lee, W.-Y.; Liang, L.-C. *Dalton Trans*. **2005**, 1952–1956.
(5) Liang, L.-C.; Lin, J.-M.; Hung, C.-H. *Organometallics* **2003**, *22*, 3007–3009.
(6) Liang, L.-C.; Lee, W.-Y.; Hung, C.-H. *Inorg. Chem*. **2003**, *42*, 5471–5473.
(7) Liang, L.-C.; Huang, M.-H.; Hung, C.-H. *Inorg. Chem*. **2004**, *43*, 2166–2174.
(8) Liang, L.-C.; Lee, W.-Y.; Yin, C.-C. *Organometallics* **2004**, *23*, 3538–3547.
(9) Liang, L.-C.; Chien, P.-S.; Huang, M.-H. *Organometallics* **2005**, *24*, 353–357.
(10) Liang, L.-C.; Lin, J.-M.; Lee, W.-Y. *Chem. Commun*. **2005**, 2462–2464.
(11) Liang, L.-C.; Chien, P.-S.; Lin, J.-M.; Huang, M.-H.; Huang, Y.-L.; Liao, J.-H. *Organometallics* **2006**, *25*, 1399–1411.
(12) Liang, L.-C.; Chien, P.-S.; Huang, Y.-L. *J. Am. Chem. Soc*. **2006**, *128*, 15562–15563.
(13) Chang, Y.-N.; Liang, L.-C. *Inorg. Chim. Acta* **2007**, *360*, 136–142.
(14) Liang, L.-C.; Chang, Y.-N.; Lee, H. M. *Inorg. Chem*. **2007**, *46*, 2666–2673.
(15) Liang, L.-C.; Chien, P.-S.; Lee, P.-Y.; Lin, J.-M.; Huang, Y.-L. *Dalton Trans*. **2008**, 3320–3327.
(16) Liang, L.-C.; Chien, P.-S.; Lee, P.-Y. *Organometallics* **2008**, *27*, 3082–3093.
(17) Liang, L.-C.; Chang, Y.-N.; Chen, H.-S.; Lee, H. M. *Inorg. Chem*. **2007**, *46*, 7587–7593.
(18) Lee, P.-Y.; Liang, L.-C. *Inorg. Chem*. **2009**, *48*, 5480−5487.
(19) Ohki, Y.; Fryzuk, M. D. *Angew. Chem., Int. Ed*. **2007**, *46*, 3180–3183.
(20) Morello, L.; Yu, P. H.; Carmichael, C. D.; Patrick, B. O.; Fryzuk, M. D. *J. Am. Chem. Soc*. **2005**, *127*, 12796–12797.
(21) Fryzuk, M. D.; Johnson, S. A.; Rettig, S. J. *J. Am. Chem. Soc*. **1998**, *120*, 11024–11025.
(22) Fryzuk, M. D.; Johnson, S. A.; Patrick, B. O.; Albinati, A.; Mason, S. A.; Koetzle, T. F. *J. Am. Chem. Soc*. **2001**, *123*, 3960–3973.
(23) MacLachlan, E. A.; Hess, F. M.; Patrick, B. O.; Fryzuk, M. D. *J. Am. Chem. Soc*. **2007**, *129*, 10895–10905.
(24) Spencer, L. P.; MacKay, B. A.; Patrick, B. O.; Fryzuk, M. D. *Proc. Natl. Acad. Sci. U.S.A*. **2006**, *103*, 17094–17098.
(25) MacKay, B. A.; Munha, R. F.; Fryzuk, M. D. *J. Am. Chem. Soc*. **2006**, *128*, 9472–9483.
(26) Studt, F.; MacKay, B. A.; Johnson, S. A.; Patrick, B. O.; Fryzuk, M. D.; Tuczek, F. *Chem.—Eur. J*. **2005**, *11*, 604–618.

Published on Web 06/11/2009

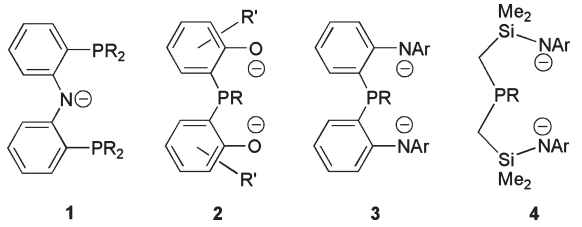

Figure 1. Representative hybrid chelating ligands.

are closely related given that both possess potentially identical hapticity, formal anionic charge, possible π-donor characteristic, and *o*-arylene backbone, although the former are anticipated to be somewhat less sterically hindered because of the lack of substituents at the anionic donor atoms.

Complexes of chelating (poly)phenolate ligands continue to constitute an active area of exploratory research to date.[27−39] We recently reported the preparation and structural characterization of group 1, 4, and 14 metal complexes of **2**.[13,14,17] For instance, the reaction of 2,2′-phenylphosphino-bis(4,6-di-*tert*-butylphenol) (H_2[OPO]) with $SnCl_4$ in the presence of NEt_3 led to the isolation of {[OPO]$SnCl_3$}($HNEt_3$) instead of [OPO]$SnCl_2$.[17] The selective formation of the monoanionic {[OPO]MX_3}$^-$ derived from a formally tetravalent metal appears to imply the synthetic possibility of a neutral [OPO]MX_3 from a formally pentavalent metal. In this regard, we have set out to prepare tantalum complexes of [OPO]$^-$ in an effort to assess this hypothesis and to pursue our interests in dinitrogen chemistry. Though this goal is yet to be achieved, we found that tantalum derivatives of [OPO]$^-$ characterized thus far preferentially adopt a bis-ligand formulation that is analogous to what was observed for heavier group 4 metals. In this contribution, we describe the preparation and structural characterization of $[OPO]_2$TaX (X = Cl, H, Me, Et, OH). Interestingly, the structure of $[OPO]_2$TaH is markedly different from those of $[OPO]_2$TaX (X = Cl, Me, Et, OH) on the basis of NMR, X-ray, and density functional theory (DFT) studies.

Results and Discussion

Though several synthetic strategies were attempted, the desired complexes of the type [OPO]TaX_3 (X = halide, alkyl) have thus far been elusive. This result is somewhat surprising in view of the successful preparation of methylene-bridged biphenolate analogues such as $[OCH_2O]TaX_3$ ($[OCH_2O]^{2-}$ = 2,2′-methylenebis(6-*tert*-butyl-4-methylphenolate), X = Cl,[40] NMe_2,[40] Me;[41] $[OCH_2O]^{2-}$ = 2,2′-methylenebis(6-phenylphenolate), X = Cl).[42] The reaction of Li_2[OPO][13] with $TaCl_5$, regardless of the molar ratio employed, in a variety of solvents produced $[OPO]_2$TaCl as the only isolable product. Prior to complete production of $[OPO]_2$TaCl, an intermediate, presumably [OPO]$TaCl_3$,[43] was observed by $^{31}P\{^1H\}$ NMR spectroscopy at about 32 ppm. Attempts to isolate this intermediate were not successful. Treatment H_2[OPO] with $TaCl_5$ gave similar results. The reactions of Li_2[OPO] with $TaMe_3Cl_2$,[44] $[OPO]_2$TaCl with $TaCl_5$, or H_2[OPO] with Ta$(CH_2Ph)_5$,[45−47] however, led to intractable products that could not be identified thus far.

Analytically pure $[OPO]_2$TaCl is readily prepared quantitatively from the reaction of Li_2[OPO][13] with $TaCl_5$ in a 2:1 ratio (Scheme 1). The room-temperature NMR data are all consistent with C_{2v} symmetry for this molecule. The $^{31}P\{^1H\}$ NMR spectrum reveals a sharp singlet resonance at 37.0 ppm for the phosphorus donors. The *tert*-butyl groups are observed as one broad and one sharp singlet resonances at 1.68 and 1.07 ppm, respectively, in the ^1H NMR spectrum at room temperature. These signals sharpen significantly upon heating (in toluene-d_8) to temperatures higher than 60 °C but resolve to give four singlet resonances upon cooling to −70 °C, indicating a rapid fluxional process occurs at elevated temperatures, and the static structure is C_2-symmetric. A similar phenomenon was also observed in the NMR studies of 7-coordinate $[OPO]_2M(OH_2)$ (M = Zr, Hf).[14] Given the non-dissociative characteristic of the phosphorus donors in Ti$[OPO]_2$ and $[OPO]_2M(OH_2)$ (M = Zr, Hf),[14] the fluxional process of $[OPO]_2$TaCl is likely to proceed by a turnstile rearrangement (Scheme 2) assuming the phosphorus does not dissociate. The non-dissociative mechanism is further supported by a negative entropy of activation (see Supporting Information) derived from peak separation analysis of the variable-temperature ^1H NMR data. Consistent with the relative size of Ta(V) versus M(IV) (M = Zr, Hf), the fluxional rate is slower for $[OPO]_2$TaCl than for $[OPO]_2M(OH_2)$ (Mz = Zr, Hf) because of intramolecular steric congestion arisen from the corresponding ligands involved.

Yellow crystals of $[OPO]_2$TaCl suitable for X-ray diffraction analysis were grown from a concentrated toluene/THF solution at −35 °C. Crystallographic details are summarized in Supporting Information, Table S1. As depicted in Figure 2, $[OPO]_2$TaCl is a 7-coordinate species that contains two facially bound [OPO]$^-$ ligands. In agreement with the

(27) Meppelder, G. J. M.; Beckerle, K.; Manivannan, R.; Lian, B.; Raabe, G.; Spaniol, T. P.; Okuda, J. *Chem. Asian J.* **2008**, *3*, 1312–1323.
(28) Gendler, S.; Zelikoff, A. L.; Kopilov, J.; Goldberg, I.; Kol, M. *J. Am. Chem. Soc.* **2008**, *130*, 2144–2145.
(29) Singh, R.; Czekelius, C.; Schrock, R. R.; Muller, P.; Hoveyda, A. H. *Organometallics* **2007**, *26*, 2528–2539.
(30) Matsuo, T.; Kawaguchi, H. *Inorg. Chem.* **2007**, *46*, 8426–8434.
(31) Agapie, T.; Bercaw, J. E. *Organometallics* **2007**, *26*, 2957–2959.
(32) Yeori, A.; Goldberg, I.; Shuster, M.; Kol, M. *J. Am. Chem. Soc.* **2006**, *128*, 13062–13063.
(33) Tsang, W. C. P.; Jamieson, J. Y.; Aeilts, S. L.; Hultzsch, K. C.; Schrock, R. R.; Hoveyda, A. H. *Organometallics* **2004**, *23*, 1997–2007.
(34) Kim, Y.; Jnaneshwara, G. K.; Verkade, J. G. *Inorg. Chem.* **2003**, *42*, 1437–1447.
(35) Kawaguchi, H.; Matsuo, T. *J. Am. Chem. Soc.* **2003**, *125*, 14254–14255.
(36) Capacchione, C.; Proto, A.; Ebeling, H.; Mulhaupt, R.; Moller, K.; Spaniol, T. P.; Okuda, J. *J. Am. Chem. Soc.* **2003**, *125*, 4964–4965.
(37) Zhu, S. S.; Cefalo, D. R.; La, D. S.; Jamieson, J. Y.; Davis, W. M.; Hoveyda, A. H.; Schrock, R. R. *J. Am. Chem. Soc.* **1999**, *121*, 8251–8259.
(38) Alexander, J. B.; La, D. S.; Cefalo, D. R.; Hoveyda, A. H.; Schrock, R. R. *J. Am. Chem. Soc.* **1998**, *120*, 4041–4042.
(39) van der Linden, A.; Schaverien, C. J.; Meijboom, N.; Ganter, C.; Orpen, A. G. *J. Am. Chem. Soc.* **1995**, *117*, 3008–3021.
(40) Chisholm, M. H.; Huang, J. H.; Huffman, J. C.; Streib, W. E.; Tiedtke, D. *Polyhedron* **1997**, *16*, 2941–2949.
(41) Watanabe, T.; Matsuo, T.; Kawaguchi, H. *Inorg. Chem.* **2006**, *45*, 6580–6582.
(42) Mulford, D. R.; Fanwick, P. E.; Rothwell, I. P. *Polyhedron* **2000**, *19*, 35–42.
(43) The reactivity of putative [OPO]$TaCl_3$ with Li_2[OPO] appears to be superior to that of $TaCl_5$ under the conditions employed, suggesting that [OPO]$TaCl_3$ be highly electrophilic.
(44) Schrock, R. R.; Sharp, P. R. *J. Am. Chem. Soc.* **1978**, *100*, 2389–2399.
(45) Schrock, R. R. *J. Organomet. Chem.* **1976**, *122*, 209–225.
(46) Groysman, S.; Goldberg, I.; Kol, M.; Goldschmidt, Z. *Organometallics* **2003**, *22*, 3793–3795.
(47) Malatesta, V.; Ingold, K. U.; Schrock, R. R. *J. Organomet. Chem.* **1978**, *152*, C53–C56.

Scheme 1

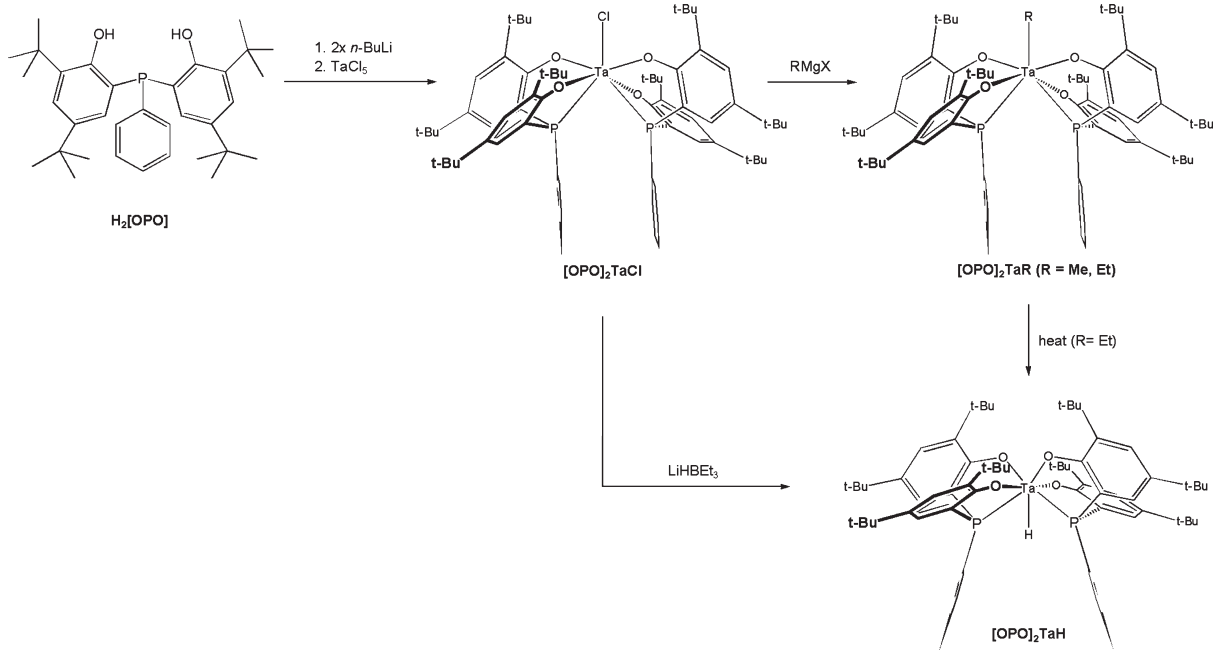

Scheme 2

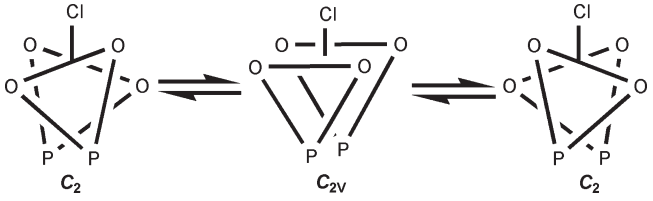

solution structure determined by NMR studies, $[OPO]_2TaCl$ is C_2-symmetic in the solid state. The principal axis coincides with the Ta−Cl bond. The geometry is best described as a distorted pentagonal bipyramid with O(1) and O(3) atoms being at the apical positions (O(1)−Ta(1)−O(3) = 154.7(3)°). The mean deviation of the equatorial pentagon is 0.2068 Å. Nevertheless, the tantalum atom lies approximately on the mean equatorial plane with negligible displacement of 0.0106 Å. The Ta−P distances of 2.714(3) Å and 2.659(3) Å in $[OPO]_2TaCl$ are slightly shorter than the M−P distances in $[OPO]_2M(OH_2)$ (2.795(2) Å and 2.757(2) Å for M = Zr; 2.723(5) Å and 2.695(4) Å for M = Hf),[14] as anticipated from the viewpoint of the relative sizes of these metals, but comparable to those of tantalum phosphine complexes such as $[NPN]TaMe_3$ (2.7713(13) Å; $[NPN]^{2-}$ = $[PhP(CH_2SiMe_2NPh)_2]^{2-}$),[21,22] $Ta(OC_6H_3{}^iPr_2\text{-}2,6)_2(Cl)_2(H)(PMe_2Ph)_2$ (2.647(1) Å),[48] $Ta(OC_6H_3{}^tBu_2\text{-}2,6)_2Cl(H)_2(PMePh_2)$ (2.655(1) Å),[48] and $[PNP]TaF_4$ (2.6556(11) and 2.6663(11) Å; $[PNP]^-$ = $[(2\text{-}{}^iPr_2P\text{-}4\text{-}MeC_6H_3)_2N]^-$).[49] The P(2)−Ta(1)−P(1) angle of 74.53(10)° is sharper than the corresponding values found for $[OPO]_2Zr(OH_2)$ (81.29(5)°) and $[OPO]_2Hf(OH_2)$ (79.7(1)°).[14]

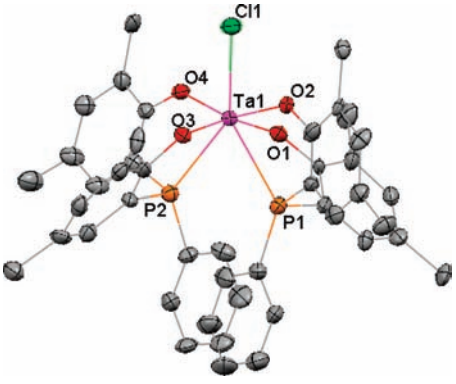

Figure 2. Molecular structure of $[OPO]_2TaCl$ with thermal ellipsoids drawn at the 35% probability level. The methyl groups in $[OPO]^{2-}$ are omitted for clarity.

Alkylation of $[OPO]_2TaCl$ with MeMgBr or EtMgCl in diethyl ether at −35 °C generated $[OPO]_2TaR$ (R = Me, Et) in high isolated yield (Scheme 1). Similar to $[OPO]_2TaCl$, both $[OPO]_2TaMe$ and $[OPO]_2TaEt$ display solution C_{2v} symmetry at room temperature on the NMR time scale but C_2 symmetry at temperatures lower than −60 °C as evidenced by variable-temperature ^1H NMR studies (in toluene-d_8). As a result, the solution structures of $[OPO]_2TaMe$ and $[OPO]_2TaEt$ are likely analogous to that of $[OPO]_2TaCl$, so is the proposed fluxional process. The $^{31}P\{^1H\}$ NMR spectra of $[OPO]_2TaMe$ and $[OPO]_2TaEt$ exhibit a sharp singlet resonance at 26.7 and 24.9 ppm, respectively, for the phosphorus donors. The C_α atom in $[OPO]_2TaMe$ and $[OPO]_2TaEt$ appears as a triplet resonance at 64.2 ppm ($^2J_{CP}$ = 17 Hz) and 74.6 ppm ($^2J_{CP}$ = 17 Hz), respectively, in the $^{13}C\{^1H\}$ NMR spectra, consistent with coordination of both phosphorus donors to the tantalum center in these 7-coordinate species.

The ethyl complex decomposes slowly upon prolonged heating at 120 °C in benzene over a course of 30 days to give $[OPO]_2TaH$ quantitatively (Scheme 1). The disappearance of $[OPO]_2TaEt$ follows a first-order rate law ($k = 2 \times 10^{-6}$ s^{-1}).

(48) Parkin, B. C.; Clark, J. R.; Visciglio, V. M.; Fanwick, P. E.; Rothwell, I. P. *Organometallics* **1995**, *14*, 3002–3013.
(49) Gerber, L. C. H.; Watson, L. A.; Parkin, S.; Weng, W.; Foxman, B. M.; Ozerov, O. V. *Organometallics* **2007**, *26*, 4866–4868.

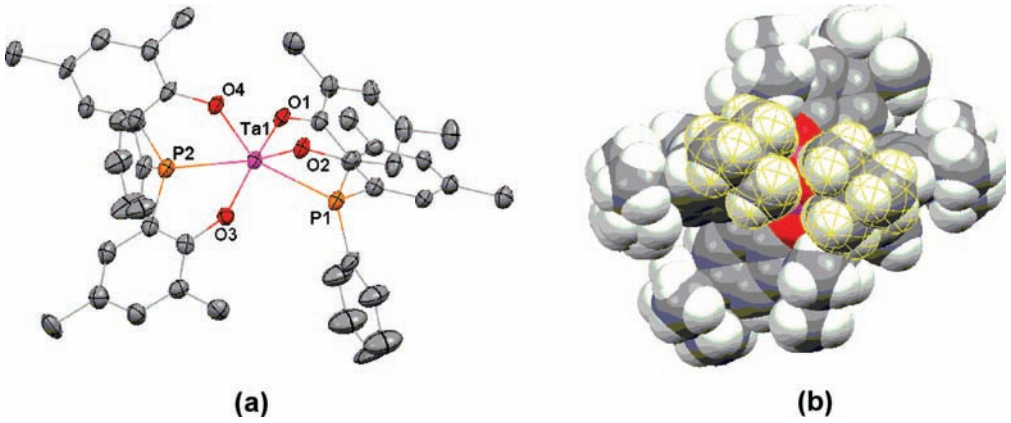

Figure 3. (a) Molecular structure of $[OPO]_2TaH$ with thermal ellipsoids drawn at the 35% probability level. The methyl groups in $[OPO]^{2-}$ are omitted for clarity. (b) A spacefill model viewed along the C_2 axis, highlighting the spatial orientation of the *tert*-butyl groups *ortho* to O(2) and O(4) donors.

Scheme 3

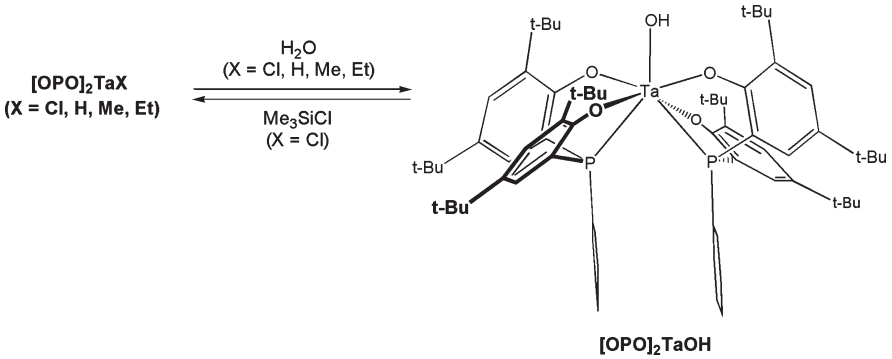

The hydride complex $[OPO]_2TaH$ can be alternatively prepared by treatment of $[OPO]_2TaCl$ with $LiHBEt_3$ in diethyl ether at −35 °C. No reaction was found for $[OPO]_2TaH$ with ethylene or 1-hexene. Interestingly, the solution NMR data of $[OPO]_2TaH$ at room temperature are consistent with C_2 symmetry, which is notably different from that of chloride and alkyl analogues. For instance, four sets of resonances are observed for the *tert*-butyl groups in the $^{13}C\{^1H\}$ NMR spectrum of $[OPO]_2TaH$ at room temperature. The solution structure of $[OPO]_2TaH$ is thus likely dissimilar from those of chloride and alkyl derivatives. The ^1H NMR spectrum of $[OPO]_2TaH$ exhibits a triplet resonance for the hydride ligand at 19.19 ppm with $^2J_{HP}$ of 74.5 Hz.[50] Similar downfield chemical shifts[22,25,48,51] and coupling constants[48,51,52] were also reported for other phosphine-coordinated tantalum hydride complexes. The $^{31}P\{^1H\}$ NMR spectrum exhibits a singlet resonance at 34.9 ppm for the phosphorus donors.

Yellow crystals of $[OPO]_2TaH$ suitable for X-ray diffraction analysis were grown from a concentrated diethyl ether solution at −35 °C. Figure 3 illustrates the X-ray structure of $[OPO]_2TaH$. Though the hydride ligand was not located experimentally, the P(2)−Ta(1)−P(1) angle of 132.48(7)° is rather large, suggesting the presence of such ligand in between the two phosphorus donors. In comparison, the P−M−P angles of $[OPO]_2TaCl$ and the six-coordinate Ti $[OPO]_2$ are 74.53(10)° and 89.93(4)°,[14] respectively. The coordination geometry of $[OPO]_2TaH$ is thus best described as a distorted pentagonal bipyramid with O(1) and O(3) atoms being at the apical positions (O(1)−Ta(1)−O(3) = 163.8(2)°). The hydride ligand resides on the principal C_2 axis. Notably, the *tert*-butyl groups *ortho* to equatorial O(2) and O(4) atoms are rather close to each other (Figure 3b). The fact that $[OPO]_2TaX$ (X = Cl, Me, Et) prefers not to adopt the same conformation as $[OPO]_2TaH$ is likely a consequence of the larger steric demand of the X ligand, which would lead instead to a wider P−Ta−P angle and thus a destabilizing close contact between the *tert*-butyl groups *ortho* to the equatorial oxygen atoms. The lack of symmetry planes in the solution structure of $[OPO]_2TaH$ at room temperature is ascribed to a similar destabilizing contact for the *ortho tert*-butyl groups in the presumed C_{2v} transition state, assuming a turnstile mechanism also proceeds. The Ta−P distances of 2.579(2) Å and 2.588(2) Å in $[OPO]_2TaH$ are shorter than those of $[OPO]_2TaCl$.

Treatment of $[OPO]_2TaCl$, $[OPO]_2TaH$, or $[OPO]_2TaR$ (R = Me, Et) with water gave $[OPO]_2TaOH$ as pale yellow crystals. The reaction of $[OPO]_2TaOH$ with Me_3SiCl afforded $[OPO]_2TaCl$ quantitatively (Scheme 3). A variable-temperature ^1H NMR study revealed solution C_{2v} symmetry for $[OPO]_2TaOH$ (toluene-d_8) at room temperature but C_2 at temperatures lower than −70 °C, similar to what is found for $[OPO]_2TaX$ (X = Cl, Me, Et) rather than $[OPO]_2TaH$. The solution structure of $[OPO]_2TaOH$ is thus analogous to those

(50) A computational study shows a distance of 2.538 Å between the hydride ligand and both phosphorus atoms, which is too far (typical H−P bond distances are ca. 1.4 Å) and thus unlikely for coupling through space.

(51) Fellmann, J. D.; Turner, H. W.; Schrock, R. R. *J. Am. Chem. Soc.* **1980**, *102*, 6608–6609.

(52) Fryzuk, M. D.; Johnson, S. A.; Rettig, S. J. *J. Am. Chem. Soc.* **2001**, *123*, 1602–1612.

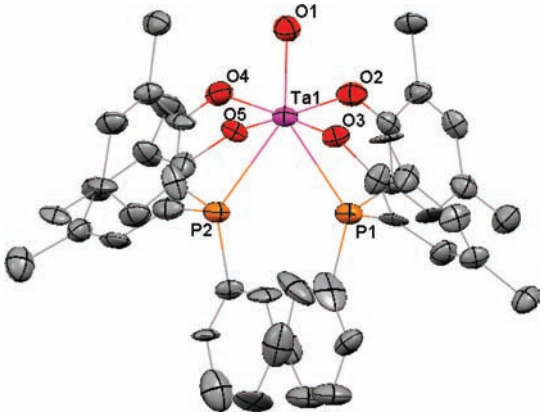

Figure 4. Molecular structure of $[OPO]_2TaOH$ with thermal ellipsoids drawn at the 35% probability level. The methyl groups in $[OPO]^{2-}$ are omitted for clarity.

of $[OPO]_2TaX$ (X = Cl, Me, Et) instead of $[OPO]_2TaH$. The hydroxide ligand of $[OPO]_2TaOH$ shows a triplet resonance in the ^1H NMR spectrum at 8.45 ppm with $^3J_{PH}$ of 4 Hz, consistent with the coordination of both phosphorus donors in this 7-coordinate species. The phosphorus donors display a singlet resonance at 25.4 ppm in the $^{31}P\{^1H\}$ NMR spectrum.

Pale yellow crystals of $[OPO]_2TaOH$ suitable for X-ray diffraction analysis were grown from a concentrated toluene solution at −35 °C. Figure 4 illustrates the X-ray structure of $[OPO]_2TaOH$. Consistent with the solution NMR studies, the solid-state structure of $[OPO]_2TaOH$ is similar to that of $[OPO]_2TaCl$ rather than $[OPO]_2TaH$. In particular, the P(1)−Ta(1)−P(2) angle of 74.20(12)° and the Ta−P distances of 2.703(4) Å and 2.718(4) Å in $[OPO]_2TaOH$ are comparable to the corresponding values of $[OPO]_2TaCl$ instead of $[OPO]_2TaH$.

DFT computations were attempted to elucidate the structural preferences for $[OPO]_2TaCl$, $[OPO]_2TaOH$, and $[OPO]_2TaH$ over two conformers as established by X-ray crystallographic studies. The optimized geometrical parameters agree reasonably well with the experimental data though the Ta−P distances of $[OPO]_2TaCl$ and $[OPO]_2TaOH$ found by DFT are somewhat overestimated (Supporting Information, Table S2). The relative energies, enthalpies, and Gibbs free energies are summarized in Supporting Information, Table S3. Notably, conformer A is appreciably lower in energy for $[OPO]_2TaOH$ than conformer B. A similar conformational preference is also found for $[OPO]_2TaCl$ though the energy differences are not as substantial as those of $[OPO]_2TaOH$. In contrast, $[OPO]_2TaH$ preferentially adopts conformer B that is lower in energy by about 7 kcal/mol than conformer A. We suggest that conformer B be electronically more favorable for complexes of the type $[OPO]_2TaX$ (X = H, Cl, Me, Et, OH) in view of the argument that Alcock's secondary bonds[53] (e.g., Ta−P bonds in this study) are less stereochemically active than primary bonds (e.g., Ta−O and Ta-X in this study) in dictating the primary coordination geometry. A similar phenomenon was also reported for $Ta(OC_6H_3{}^tBu_2\text{-}2,6)_2(Cl)(H)_2(PMePh_2)$[48] and other main group[54,55] and transition metal complexes.[56,57] Incorporation of a sterically more demanding X ligand, for example, Cl, Me, Et, or OH, however, increases the steric congestion significantly (vide supra) and thus conformer A becomes favorable.

Conclusions

In summary, we have prepared a series of tantalum complexes of the tridentate biphenolate phosphine ligand $[OPO]^{2-}$ and established the solution and solid-state structures of these molecules by means of multinuclear NMR spectroscopy and X-ray crystallography. These compounds preferentially adopt a bis-ligand conformation of the type $[OPO]_2TaX$ due perhaps to the high electrophilicity of the presumed $[OPO]TaX_3$. The coordination geometry is best described as a distorted pentagonal bipyramid for all isolated derivatives. Of particular note is perhaps the divergent preference for the coordination structure, which is a function of the identity of the monoanionic X ligand. Specifically, $[OPO]_2TaH$ adopts a structure that is notably different from $[OPO]_2TaCl$, $[OPO]_2TaOH$, $[OPO]_2TaMe$, and $[OPO]_2TaEt$ on the basis of NMR, X-ray, and DFT studies.

Experimental Section

General Procedures. Unless otherwise specified, all experiments were performed under nitrogen using standard Schlenk or glovebox techniques. All solvents were reagent grade or better and purified by standard methods. The NMR spectra were recorded on Varian Unity or Bruker AV instruments. Chemical shifts (δ) are listed as parts per million downfield from tetramethylsilane and coupling constants (J) in hertz. ^1H NMR spectra are referenced using the residual solvent peak at δ 7.16 for C_6D_6. ^{13}C NMR spectra are referenced using the residual solvent peak at δ 128.39 for C_6D_6. The assignment of the carbon atoms is based on the DEPT ^{13}C NMR spectroscopy. ^{31}P NMR spectra are referenced externally using 85% H_3PO_4 at δ 0. Routine coupling constants are not listed. All NMR spectra were recorded at room temperature in specified solvents unless otherwise noted. Elemental analysis was performed on a Heraeus CHN-O Rapid analyzer.

Materials. Compounds $H_2[OPO]$[58] and $Li_2[OPO]$[13] were prepared according to the literature procedures. All other chemicals were obtained from commercial vendors and used as received.

X-ray Crystallography. Crystallographic data, selected bond distances (Å) and angles (deg) for $[OPO]_2TaCl$, $[OPO]_2TaH$, and $[OPO]_2TaOH$ are given in the Supporting Information. Data were collected on a Bruker-Nonius Kappa CCD diffractometer with graphite monochromated Mo Kα radiation (λ = 0.7107 Å). Structures were solved by direct methods and refined by full matrix least-squares procedures against F^2 using WinGX crystallographic software package or SHELXL-97.[59] All full-weight non-hydrogen atoms were refined anisotropically. Hydrogen atoms were placed in calculated positions. The crystals of $[OPO]_2TaOH$ were of poor quality but sufficient to establish the identity of this molecule. The structures of $[OPO]_2TaCl$, $[OPO]_2TaH$, and $[OPO]_2TaOH$ contain disordered THF, diethyl ether, and toluene molecules, respectively. Attempts to obtain a suitable disorder model failed. The SQUEEZE procedure of

(53) Alcock, N. W. *Adu. Inorg. Chem. Radiochem.* **1972**, *15*, 1.
(54) Haaland, A. *Angew. Chem., Int. Ed. Engl.* **1989**, *28*, 992–1007.
(55) Goel, S. C.; Chiang, M. Y.; Buhro, W. E. *J. Am. Chem. Soc.* **1990**, *112*, 6724–6725.
(56) Kobriger, L. M.; McMullen, A. K.; Fanwick, P. E.; Rothwell, I. P. *Polyhedron* **1989**, *8*, 77–81.
(57) Fryzuk, M. D.; Carter, A.; Rettig, S. J. *Organometallics* **1992**, *11*, 469–472.
(58) Siefert, R.; Weyhermuller, T.; Chaudhuri, P. *J. Chem. Soc., Dalton Trans.* **2000**, 4656–4663.
(59) Sheldrick, G. M. *SHELXTL*, Version 5.1; Bruker AXA Inc.: Madison, WI, 1998.

Platon program[60] was used to obtain a new set of F^2 (*hkl*) values without the contribution of solvent molecules, leading to the presence of significant voids in these structures. The refinement reduced R1 values of $[OPO]_2TaCl$, $[OPO]_2TaH$, and $[OPO]_2$-TaOH to 0.0873, 0.0719, and 0.1116, respectively.

DFT Computations. The three-parameter hybrid of exact exchange and Becke's exchange energy functional[61] and Lee−Yang−Parr's gradient-corrected correlation energy functional[62] (B3LYP) were used. X-ray crystallographic data were employed to initiate the optimizations of molecular geometries. All optimized structures were verified to be genuine minima on the potential energy surface via vibrational frequency analysis. The 6-31G basis sets were used for C, H, O, Cl, P and the LANL2DZ effective core potential plus basis functions for Ta.[63] The Gaussian03 suite of programs was applied in this study.[64]

Synthesis of $[OPO]_2TaCl$. Method 1. Solid $H_2[OPO]$ (297.9 mg, 0.58 mmol) was dissolved in diethyl ether (6 mL) and cooled to −35 °C. To this was added *n*-BuLi (0.46 mL, 2.5 M in hexane, Aldrich, 1.15 mmol, 2 equiv) dropwise. The reaction mixture was stirred at room temperature for 1 h. The resultant solution was cooled to −35 °C again and added dropwise to a pre-chilled suspension of $TaCl_5$ (103.0 mg, 0.29 mmol) in diethyl ether (120 mL) at −35 °C. The reaction mixture was stirred at room temperature for 7 d and filtered through a pad of Celite. Evaporation of the filtrate in vacuo to dryness afforded the product as a yellow solid; yield 358.2 mg (99.7%). Yellow crystals suitable for X-ray diffraction analysis were grown from a concentrated toluene/THF solution at −35 °C; yield 201 mg (56%).

Method 2. Trimethylsilyl chloride (30.2 mg, 0.28 mmol) was added to a diethyl ether solution (10 mL) of $[OPO]_2TaOH$ (342.6 mg, 0.28 mmol) at room temperature. The reaction solution was stirred at room temperature for 1 h and evaporated to dryness under reduced pressure to afford the product as a yellow solid; yield 332 mg (96%). ^1H NMR (C_6D_6, 500 MHz) δ 7.47 (br s, 4, Ar), 7.16 (br s, 4, Ar), 6.95 (m, 4, Ar), 6.83 (t, 2, Ar), 6.69 (t, 4, Ar), 1.68 (br s, 36, C*Me*$_3$), 1.07 (s, 36, C*Me*$_3$). $^{31}P\{^1H\}$ NMR (C_6D_6, 202.31 MHz) δ 37.02. $^{13}C\{^1H\}$ NMR (C_6D_6, 125.70 MHz) δ 168.00 (m, C), 144.56 (t, J_{CP} = 2.77, C), 140.21 (t, J_{CP} = 2.26, C), 133.87 (t, J_{CP} = 22.59, CH), 129.96 (s, CH), 129.82 (m, C), 128.90 (m, CH), 128.00 (s, CH), 128.62 (s, CH), 36.13 (s, *C*Me$_3$), 34.95 (s, *C*Me$_3$), 31.96 (s, C*Me*$_3$), 30.46 (s, C*Me*$_3$). Anal. Calcd for $C_{68}H_{90}ClO_4P_2Ta$: C, 65.33; H, 7.26. Found: C, 65.37; H, 7.47

Synthesis of $[OPO]_2TaMe$. Solid $[OPO]_2TaCl$ (99.9 mg, 0.08 mmol) was dissolved in diethyl ether (3 mL) and cooled to −35 °C. To this was added MeMgBr (0.16 mL, 0.5 M in diethyl ether, 0.08 mmol) dropwise. The reaction mixture was stirred at room temperature for 2 h and filtered through a pad of Celite. The filtrate was concentrated under reduced pressure until the volume became about 2 mL. The concentrated solution was cooled to −35 °C to afford the product as greenish yellow crystals; yield 70 mg (71%). ^1H NMR (C_6D_6, 500 MHz) δ 7.46 (s, 4, Ar), 7.16 (br s, 4, Ar), 6.95 (br s, 4, Ar), 6.85 (t, 2, J = 7, Ar), 6.72 (t, 4, J = 7, Ar), 2.71 (s, 3, Ta*Me*), 1.63 (s, 36, C*Me*$_3$), 1.10 (s, 36, C*Me*$_3$). $^{31}P\{^1H\}$ NMR (C_6D_6, 202.31 MHz) δ 26.74. $^{13}C\{^1H\}$ NMR (C_6D_6, 125.70 MHz) δ 167.87 (m, C), 143.47 (s, C), 139.12 (s, C), 133.46 (t, J_{CP} = 5.53, CH), 130.57 (m, C), 129.17 (s, CH), 128.67 (t, CH), 127.78 (s, CH), 126.44 (br s, CH), 123.64 (m, C), 64.23 (t, $^2J_{CP}$ = 17.47, Ta*Me*), 35.87 (s, *C*Me$_3$), 34.77 (s, *C*Me$_3$), 31.87 (s, C*Me*$_3$), 30.33 (s, C*Me*$_3$). Anal. Calcd for $C_{69}H_{93}O_4P_2Ta$: C, 67.39; H, 7.63. Found: C, 67.33; H, 7.72.

Synthesis of $[OPO]_2TaEt$. Procedures are essentially the same as those of $[OPO]_2TaMe$ by using EtMgCl to give a yellow crystalline solid; yield 71%. ^1H NMR (C_6D_6, 500 MHz) δ 7.46 (m, 4, Ar), 7.16 (br s, 4, Ar), 6.92 (dd, 4, Ar), 6.85 (t, 2, J = 7.5, Ar), 6.72 (t, 4, J = 7.5, Ar), 3.29 (br s, 2, TaC*H*$_2$CH$_3$), 3.06 (t, 3, $^3J_{HH}$ = 7.5, TaCH$_2$C*H*$_3$), 1.63 (br s, 36, C*Me*$_3$), 1.10 (s, 36, C*Me*$_3$). $^{31}P\{^1H\}$ NMR (C_6D_6, 202.31 MHz) δ 24.94. $^{13}C\{^1H\}$ NMR (C_6D_6, 125.70 MHz) δ 167.00 (m, C), 143.30 (s, C), 139.06 (s, C), 133.66 (t, J_{CP} = 5.53, CH), 130.57 (m, C), 129.10 (s, CH), 128.68 (s, CH), 128.58 (t, CH), 127.83 (s, CH), 124.00 (m, C), 74.60 (t, $^2J_{CP}$ = 17.47, Ta*C*H$_2$CH$_3$), 35.82 (s, *C*Me$_3$), 34.73 (s, *C*Me$_3$), 31.87 (s, C*Me*$_3$), 30.64 (s, C*Me*$_3$), 16.35 (s, TaCH$_2$*C*H$_3$). Anal. Calcd for ($C_{70}H_{95}O_4P_2Ta$)(toluene): C, 69.23; H, 7.78. Found: C, 68.97; H, 7.62y.

Synthesis of $[OPO]_2TaH$. Method 1. Procedures are essentially the same as those of $[OPO]_2TaR$ (R = Me, Et) by using $LiHBEt_3$ to give yellow crystals; yield 76%.

Method 2. A benzene solution (0.6 mL) of $[OPO]_2TaEt$ (19.4 mg, 0.016 mmol) was transferred to a Teflon-capped NMR tube and heated to 120 °C. The reaction was periodically monitored by $^{31}P\{^1H\}$ NMR which indicated quantitative formation of $[OPO]_2TaH$ in 30 d. ^1H NMR (C_6D_6, 500 MHz) δ 19.19 (t, 1, $^2J_{HP}$ = 74.5, Ta−H), 7.89 (dd, 4, Ar), 7.71 (d, 2, Ar), 7.65 (m, 2, Ar), 7.40 (m, 2, Ar), 7.22 (d, 2, Ar), 7.07 (t, 4, Ar), 6.96 (t, 2, Ar), 1.96 (s, 18, C*Me*$_3$), 1.26 (s, 18, C*Me*$_3$), 1.09 (s, 36, C*Me*$_3$). $^{31}P\{^1H\}$ NMR (C_6D_6, 202.31 MHz) δ 34.91. $^{13}C\{^1H\}$ NMR (C_6D_6, 125.70 MHz) δ 172.12 (m, C), 165.54 (m, C), 144.48 (t, J_{CP} = 3.65, C), 143.35 (t, J_{CP} = 2.77, C), 140.71 (t, J_{CP} = 4.53, C), 139.06 (t, J_{CP} = 2.77, C), 134.50 (t, J_{CP} = 5.53, CH), 131.31 (d, J_{CP} = 55.06, C), 130.87 (s, CH), 129.86 (m, C), 129.15 (m, CH), 129.10 (m, CH), 128.98 (s, CH), 127.81 (s, CH), 127.06 (s, CH), 118.70 (m, C), 36.84 (s, *C*Me$_3$), 35.63 (s, *C*Me$_3$), 35.04 (s, *C*Me$_3$), 35.01 (s, *C*Me$_3$), 32.29 (s, C*Me*$_3$), 32.11 (s, C*Me*$_3$), 31.21 (s, C*Me*$_3$), 30.37 (s, C*Me*$_3$). Anal. Calcd for $C_{68}H_{91}O_4P_2Ta$: C, 67.18; H, 7.55. Found: C, 66.86; H, 7.37.

Synthesis of $[OPO]_2TaOH$. Degassed deionized water (300 mg, 16.7 mmol, 415 equiv) was added to a THF solution (2 mL) of $[OPO]_2TaEt$ (50 mg, 0.0402 mmol) at room temperature. The reaction solution was stirred at room temperature for 4 d. The $^{31}P\{^1H\}$ NMR spectrum of a reaction aliquot at this moment indicated the presence of a two-component mixture containing $[OPO]_2TaOH$ and $H_2[OPO]$ in a ratio of about 4:1. All volatiles were removed in vacuo. Toluene (2 mL) was added. The toluene solution was filtered through a pad of Celite, concentrated under reduced pressure, and cooled to −35 °C to afford the product as pale yellow crystals suitable for X-ray diffraction analysis; yield 21.3 mg (43%). Reactions employing $[OPO]_2TaX$ (X = Cl, Me, H) under similar conditions gave essentially the same results as indicated by $^{31}P\{^1H\}$ NMR. ^1H NMR (C_6D_6, 500 MHz) δ 8.45 (t, 1, $^3J_{PH}$ = 4, OH), 7.45 (d, 4, J = 2, Ar), 7.16 (br s, 4, Ar), 7.00 (dd, 4, J = 10.5 and 7.5, Ar), 6.85 (t, 2, J = 7.5, Ar), 6.73 (t, 4, J = 7.5, Ar), 1.63 (br s, 36, C*Me*$_3$), 1.09 (s, 36, C*Me*$_3$). $^{31}P\{^1H\}$ NMR (C_6D_6, 202.31 MHz) δ 25.38. $^{13}C\{^1H\}$ NMR (C_6D_6, 125.70 MHz) δ 166.86 (m, C), 143.47 (t, J_{CP} = 2.77, C), 139.11 (br s, C), 133.73 (t, J_{CP} = 5.41, CH), 129.57

(60) Spek, A. L. *PLATON - A Multipurpose Crystallographic Tool*; Utrecht University: The Netherlands, 2003.
(61) Becke, A. D. *J. Chem. Phys.* **1993**, *98*, 5648–5652.
(62) Lee, C.; Yang, W.; Parr, R. G. *Phys. Rev. B* **1988**, *37*, 785–789.
(63) Hay, P. J.; Wadt, W. R. *J. Chem. Phys.* **1985**, *82*, 270–283.
(64) Frisch, M. J.; Trucks, G. W.; Schlegel, H. B.; Scuseria, G. E.; Robb, M. A.; Cheeseman, J. R.; Montgomery Jr., J. A.; Vreven, T.; Kudin, K. N.; Burant, J. C.; Millam, J. M.; Lyengar, S. S.; Tomasi, J.; Barone, V.; Mennucci, B.; Cossi, M.; Scalmani, G.; Rega, N.; Petersson, G. A.; Nakatsuji, H.; Hada, M.; Ehara, M.; Toyota, K.; Fukuda, R.; Hasegawa, J.; Ishida, M.; MNakajima, T.; Honda, Y.; Kitao, O.; Nakai, H.; Klene, M.; Li, X.; Knox, J. E.; Hratchian, H. P.; Cross, J. B.; Adamo, C.; Jaramillo, J.; Gomperts, R.; Stratmann, R. E.; Yazyev, O.; Austin, A. J.; Cammi, R.; Pomelli, C.; Ochterski, J.; Ayala, P. Y.; Morokuma, K.; Voth, G. A.; Salvador, P.; Dannenberg, J. J.; Zakrzewski, V. G.; Dapprich, S.; Daniels, A. D.; Strain, M. C.; Farkas, O.; Malick, D. K.; Rabuck, A. D.; Raghavachari, K.; Foresman, J. B.; Ortiz, J. V.; Cui, Q.; Baboul, A. G.; Clifford, S.; Cioslowski, J.; Stefanov, B. B.; Liu, G.; Liashenko, A.; Piskorz, P.; Komaromi, I.; Martin, R. L.; Fox, D. J.; Keith, T.; Al-Laham, M. A.; Peng, C. Y.; Nanayakkara, A.; Challacombe, M.; Gill, P. M. W.; Johnson, B.; Chen, W.; Wong, M. W.; Gonzalez, C.; Pople, J. A.; *Gaussian 03*, Revision B.05; Gaussian, Inc.: Pittsburgh, PA, 2003.

(s, CH), 128.90 (m, CH), 127.89 (s, CH), 123.86 (m, C), 35.82 (s, CMe_3), 34.77 (s, CMe_3), 31.88 (s, CMe_3), 30.32 (s, CMe_3). Anal. Calcd for $C_{68}H_{91}O_5P_2Ta$: C, 66.31; H, 7.45. Found: C, 66.55; H, 7.65.

Acknowledgment. We thank the National Science Council of Taiwan for financial support (NSC 96-2628-M-110-007-MY3 and 96-2918-I-110-011) of this work, Ms. Ru-Rong Wu (NCKU) for technical assistance with variable-temperature NMR experiments, Mr. Ting-Shen Kuo (NTNU) for X-ray crystallography, and the National Center for High-performance Computing (NCHC) for computer time and facilities.

Supporting Information Available: X-ray crystallographic data, DFT results, and activation parameters. This material is available free of charge via the Internet at http://pubs.acs.org.